

Figure 1. Absorption spectra in acetonitrile for $\text{Mn}^{\text{IV}}(\text{DTBC})_3^{2-}$ [prepared in situ by the combination of $\text{Mn}^{\text{II}}(\text{DMU})_6(\text{ClO}_4)_2$ (DMU = dimethylurea), 3,5-di-*tert*-butylcatechol (DTBC $_2$), tetraethylammonium hydroxide ((TEA)OH), and 3,5-di-*tert*-butyl-*o*-benzoquinone (DTBQ) in a mole ratio of 1:2:4.6:1]^{2,6} under a purified N_2 (1 atm) atmosphere (spectrum a), after the solution is bubbled with O_2 (1 atm) for 1 min at 0 °C (spectrum b), after the preceding solution is purged with Ar for 1 min at 0 °C (spectrum c), and after the preceding solution is purged with Ar for 10 min at 0 °C (spectrum d). The spectrum for the product solution that results (10 min after preparation) from the combination of 1 mM DTBQ and 6 mM (TEA)OH in acetonitrile (Ar, 1 atm) is presented for comparison (spectrum e). The apparent molar absorptivities (ϵ) represent the observed absorbances divided by the initial concentrations of $\text{Mn}^{\text{IV}}(\text{DTBC})_3^{2-}$ (0.1 mM) for curves a–d and by the initial concentration of DTBQ (1 mM) for curve e.

nate(IV) complex, $\text{Mn}^{\text{IV}}(\text{DTBC})_3^{2-}$ in acetonitrile (CH_3CN) to reversible binding of dioxygen by the complex. Cooper and Hartman¹ conclude that the dominant process is an irreversible oxidation by oxygen of bound DTBC to give the *o*-quinone (DTBQ), which subsequently undergoes a Michael addition under alkaline conditions to give a brown, insoluble polymer. In support of this interpretation they present a spectrum (Figure 3)¹ for the product from the degradation of 3,5-di-*tert*-butyl-*o*-benzoquinone (DTBQ) in an alkaline Me_2SO solution.

To give the reader quantitative perspective, we have repeated the spectrophotometric experiments of Magers, Smith, and Sawyer.^{2,3} The resultant spectra for $\text{Mn}^{\text{IV}}(\text{DTBC})_3^{2-}$ (a) in slightly basic acetonitrile (1 atm of Ar), (b) after oxygenation (1 atm of O_2) for 1 min, (c) after the preceding solution is purged for 1 min with argon, and (d) after the preceding solution is purged for 10 min with argon are compared in Figure 1. The presence of isosbestic points at 370 and 510 nm is consistent with an equilibrium process rather than with irreversible degradation (there is no evidence for any precipitate). For direct quantitative comparison, the spectrum for an alkaline solution of DTBQ (recorded 10 min after its preparation) is included in Figure 1. The spectrum for the latter solution (i) does not compare qualitatively or quantitatively with that for the O_2 adduct of $\text{Mn}^{\text{IV}}(\text{DTBC})_3^{2-}$, (ii) is not reversible, and (iii) does not undergo a significant increase in absorbance at 440 nm for a period up to 50 h.

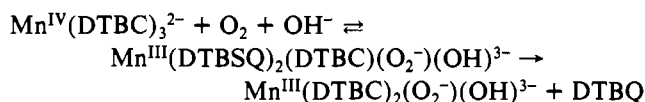
As observed previously,^{2,3} the oxygenation–deaeration cycle for $\text{Mn}^{\text{IV}}(\text{DTBC})_3^{2-}$ in acetonitrile is reversible; the respective absorption spectra diminish less than 5% per cycle. In contrast to the observation of the preceding note,¹ we do not observe a change from green to red-brown during the first 10 h after preparation of the alkaline DTBQ solution of Figure 1.

In response to the suggestion that the apparent reversibility is actually due to decomposition of the oxygenated complex,¹ we find that the spectrum for the solution of Figure 1b (the oxygen adduct) remains virtually unchanged for at least 2 h in a sealed cell at 0 °C.

The primary thesis of the reappraisal¹ (i.e., oxidation by molecular oxygen of the bound DTBC ligands of $\text{Mn}^{\text{IV}}(\text{DTBC})_3^{2-}$ to give DTBQ) is not supported by the redox thermodynamics. A recent paper⁴ demonstrates that the reversible redox potential for oxidation of $\text{Mn}^{\text{IV}}(\text{DTBC})_3^{2-}$ in CH_3CN is approximately –0.4 V vs. SCE (between –0.1 and –0.6 V vs. SCE); the redox potential for reduction of O_2 is –1.0 V vs. SCE in acetonitrile.⁵ The cyclic voltammetric oxidation potential for the $\text{Mn}^{\text{IV}}(\text{DTBC})_3^{2-}$ complex under the solution conditions of Figure 1a is –0.2 V vs. SCE at 0 °C. Thus, the purported primary reaction [$\text{O}_2 + \text{Mn}^{\text{IV}}(\text{DTBC})_3^{2-} \rightleftharpoons \text{Mn}^{\text{IV}}(\text{DTBC})_2(\text{DTBSQ})^- + \text{O}_2^-$] is disfavored by –0.6 V. To have a net reaction requires stabilization of the product species by adduct formation, which can be a reversible process (Figure 1).

Conclusion

The reinterpretations and conclusions of Cooper and Hartman¹ are not supported by the experimental results. Recent studies⁶ provide additional support for the conclusion that dioxygen is reversibly bound by dilute concentrations (~0.1 mM) of $\text{Mn}^{\text{IV}}(\text{DTBC})_3^{2-}$ in slightly alkaline acetonitrile:



The fragile nature of the adduct and its instability at high temperatures, high concentrations, and in the presence of moist air or excess base were noted in the previous paper,³ as was the limitation for the reversible process to the conditions of Figure 1. The new data of the preceding note (Figures 3 and 4)¹ constitute a confirmation of these irreversible degradation processes (especially in Me_2SO solutions) but are not the basis for a rational reappraisal of the reversible oxygenation reaction.

Acknowledgment. This work was supported by the National Institutes of Health—USPHS under Grant No. GM-22761.

Registry No. $\text{Mn}^{\text{IV}}(\text{DTBC})_3^{2-}$, 72268-94-1; O_2 , 7782-44-7.

- (4) Jones, S. E.; Chin, D.-H.; Sawyer, D. T. *Inorg. Chem.* **1981**, *20*, 4257.
 (5) Sawyer, D. T.; Valentine, J. S. *Acc. Chem. Res.* **1981**, *14*, 393.
 (6) Chin, D.-H.; Sawyer, D. T.; Schaefer, W. P.; Simmons, C. J., submitted for publication in *Inorg. Chem.*

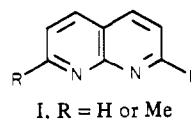
Contribution from the Department of Chemistry, University of Victoria, British Columbia, Canada V8W 2Y2

Site Exchange of Octahedral Metal Centers between Equivalent Nitrogen Atoms in Complexes of 1,8-Naphthyridine or Phthalazine: A ¹H NMR Study of Pentacarbonylchromium and -tungsten Derivatives

Keith R. Dixon,* Donald T. Eadie, and Stephen R. Stobart*

Received March 19, 1982

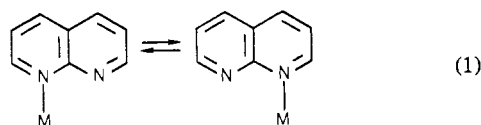
The coordination chemistry of 1,8-naphthyridines (I), es-



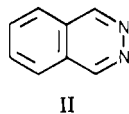
pecially the parent molecule (R = H, naph) and its 2,7-di-

methyl derivative (R = Me, dmnaph), has been extensively studied in relation to a wide variety of metal centers.¹ These heterocycles are of considerable interest as ligands because of their ability to adopt geometries ranging from fully bidentate, through various unsymmetrical structures, to essentially monodentate coordination. Thus in crystalline [Fe(naph)₄][ClO₄]₂ one ligand is an almost symmetric chelate while the others exhibit varying degrees of asymmetry.² In solid [Hg₂(naph)₂][ClO₄]₂ the ligands are bound³ via one nitrogen (Hg-N = 2.03 Å) with the second nitrogen comparatively remote (Hg-N = 2.78 Å), and even more unsymmetrical ligation occurs in [cis-PtCl(PET₃)₂(naph)][BF₄] with Pt-N distances⁴ of 2.08 and 3.05 Å. Surprisingly, in view of these results, the corresponding solution behavior where dynamic exchange of a metal center may occur between the two nitrogen atoms in I has received rather little attention; indeed, it has only been considered for complexes where the metal coordination is essentially square planar if weak coordination by the more remote naphthyridine nitrogen is ignored, viz., [AuX(CH₃)₂(dmnaph)], X = Cl, Br, I, OCN, SCN, SeCN, or CN⁵ and [cis-MCl(PR₃)₂(naph)][BF₄], M = Pt or Pd.^{6,7}

In order to investigate the generality of a dynamic process involving metal site exchange in structure I (eq 1), in relation



to octahedral coordination about a metal center, we have reexamined the solution properties of the complexes [M(CO)₅(naph)], M = Cr, Mo, and W. These compounds had been prepared previously and a dynamic process suggested on the basis of poorly resolved ambient-temperature NMR spectra,⁸ but no variable-temperature study had been reported. We have also studied the related octahedral complexes [M(CO)₅(phth)], where phth = phthalazine (II), because previous studies in square-planar systems^{6,7} have shown marked differences in metal site exchange rates compared with those of the naph analogues.



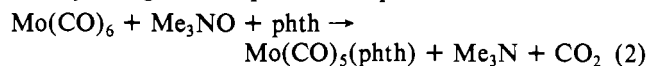
Results

1. Preparation and Infrared Spectra. The complexes [M(CO)₅L], M = Cr and W, L = naph and phth, were prepared by displacement reactions from [M(CO)₅(solvent)] species generated in situ by UV irradiation [M(CO)₆] in tetrahydrofuran (L = phth) or methanol (L = naph). The naph complexes had physical properties and IR spectra consistent with those reported previously.⁸ [Cr(CO)₅(phth)] and [W(CO)₅(phth)] were orange, air-sensitive solids, soluble in a wide range of organic solvents, mass spectra of which showed parent ions and fragments due to successive loss of five CO groups.

- (1) D. G. Hendricker and R. J. Foster, *Inorg. Chem.*, **12**, 349 (1973), and references therein; J. R. Wagner and D. G. Hendricker, *J. Inorg. Nucl. Chem.*, **37**, 1375 (1975), and references therein; R. J. Staniewicz, R. F. Sympton, and D. G. Hendricker, *Inorg. Chem.*, **16**, 2166 (1977).
- (2) A. Clearfield, P. Singh, and I. Bernal, *J. Chem. Soc. D*, 389 (1970); *J. Coord. Chem.*, **1**, 29 (1971).
- (3) J. C. Dewan, D. L. Kepert, and A. H. White, *J. Chem. Soc., Dalton Trans.*, 490 (1975).
- (4) G. W. Bushnell, K. R. Dixon, and M. A. Khan, *Can. J. Chem.*, **46**, 450 (1978).
- (5) H. Schmidbaur and K. C. Dash, *J. Am. Chem. Soc.*, **95**, 4855 (1973).
- (6) K. R. Dixon, *Inorg. Chem.*, **16**, 2618 (1977).
- (7) J. B. Brandon, M. Collins, and K. R. Dixon, *Can. J. Chem.*, **56**, 950 (1978).
- (8) T. E. Reed and D. G. Hendricker, *J. Coord. Chem.*, **2**, 83 (1972).

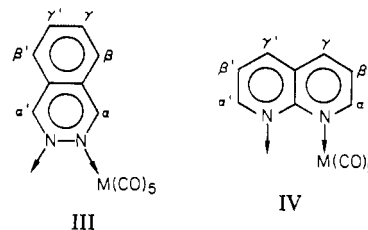
IR spectra showed four CO stretching absorptions: M = Cr (CCl₄ solution) 2062 m, 1982 m, 1938 s, 1905 m cm⁻¹; M = W (THF solution) 2071 m, 1989 m, 1942 vs, 1906 m cm⁻¹. These patterns are typical of pentacarbonyl derivatives, resembling, for example, that found⁹ for [M(CO)₅(py)]. For such a configuration under C_{4v} symmetry 2a₁ + e modes are IR active, but when the geometry of the axial ligand lowers the overall symmetry, the b₁ mode often appears as a weak absorption through relaxing of the C_{4v} selection rules.⁹ The [M(CO)₅(naph)] spectra are similar to those for the phth complexes and suggest a monodentate structure for both sets of products. This conclusion is confirmed by the NMR spectra discussed below.

In addition to the Cr and W complexes described above, we have prepared [Mo(CO)₅(phth)] by the same method and also by that given in eq 2. Mass spectra and IR and NMR



data for this Mo complex were very similar to those for the Cr and W analogues, and it clearly exhibits the same type of dynamic stereochemistry in solution. However, the compound is difficult to purify and is sensitive in solution, so that reliable rate study by variable-temperature NMR was not possible. Furthermore, we were unable to produce [Mo(CO)₅(naph)] although small yields of impure material have been obtained⁸ previously.

2. Variable-Temperature NMR Spectra. (a) Phthalazine Complexes. Ambient-temperature ¹H NMR spectra of the phth complexes [M(CO)₅(phth)] (M = Cr and W) in dioxane solution consisted of two clearly separated singlets for the α and α' protons together with a complex multiplet for the ββ'γγ' set. This supports a structure (III) with only one nitrogen



coordinated to the metal, and comparison with previous results⁶ indicates that the singlet to lower field should be assigned to α. Thus for M = Cr, δ_α = 9.61, δ_{α'} = 9.20, and δ_{ββ'γγ'} = 7.98; for M = W, δ_α = 10.12, δ_{α'} = 9.53, and δ_{ββ'γγ'} = 7.80. When the temperature is raised, α and α' resonances broaden and then coalesce to a single resonance above ~100 °C, indicating that rapid exchange of the metal is occurring between the two possible nitrogen coordination sites. Line widths in the ambient-temperature spectra (M = Cr, 3.6 Hz; M = W, 3.2 Hz) were used to establish T₂ (transverse relaxation time 1/πν_{1/2}), and rate constants (k) for the site-exchange process were obtained by computer simulation of the line shapes at various temperatures. The best straight lines obtained by linear regression analysis of Eyring plots, ln(k/T) against (1/T), were then compared with the standard transition-state theory equation (κ = Boltzmann constant)

$$\ln(k/T) = -\frac{\Delta H^\ddagger}{R}(1/T) + \frac{\Delta S^\ddagger}{R} + \ln(\kappa/h)$$

to yield the thermodynamic parameters collected in Table I.

(b) Naphthyridine Complexes. As for the phth complexes, the low-temperature limit spectra for [M(CO)₅(naph)], M = Cr or W, support a formulation in which one nitrogen atom interacts much more strongly with the metal than the other

- (9) C. S. Kraihanzel and F. A. Cotton, *Inorg. Chem.*, **2**, 535 (1963); *J. Am. Chem. Soc.*, **84**, 4432 (1962).

Table I. Summary of Dynamic ^1H NMR Data for Phthalazine and Naphthyridine Complexes

| compd | temp range, K | no. of spectra | Eyring plot ^a | | | thermodynamic parameters ^b | | |
|---------------------------------------|---------------|----------------|--------------------------|--------|-------|---|--|---|
| | | | R^2 | A | B | ΔH^{\ddagger} , kJ mol ⁻¹ | ΔS^{\ddagger} , J deg ⁻¹ mol ⁻¹ | ΔG^{\ddagger} , kJ mol ⁻¹ |
| $\text{Cr}(\text{CO})_5(\text{phth})$ | 303-398 | 16 | 0.995 | -10824 | 28.16 | 90.0 | 36.6 | 79.1 |
| $\text{W}(\text{CO})_5(\text{phth})$ | 308-408 | 16 | 0.967 | -9240 | 23.51 | 76.8 | -2.1 | 77.4 |
| $\text{Cr}(\text{CO})_5(\text{naph})$ | 243-303 | 13 | 0.994 | -6568 | 22.10 | 54.6 | -13.8 | 58.7 |
| $\text{W}(\text{CO})_5(\text{naph})$ | 233-303 | 8 | 0.991 | -7092 | 24.83 | 59.0 | 8.9 | 56.3 |

^a R^2 , A , and B are the correlation coefficient, slope, and intercept, respectively, derived from linear regression analysis of a plot of $\ln(k/T)$ against $1/T$, where k is the rate constant obtained by line shape fitting of the observed spectra. ^b Derived from the Eyring plot by assuming the following: (see Results section) $A = -\Delta H^{\ddagger}/R$; $B = \Delta S^{\ddagger}/R + \ln(k/h)$; $\Delta G^{\ddagger} = \Delta H^{\ddagger} - T\Delta S^{\ddagger}$.

Table II. ^1H NMR Parameters for 1,8-Naphthyridine Complexes

| compd | temp, °C | chem shifts, ppm ^a | | | coupling const, Hz ^a | | |
|--|----------|-------------------------------|-----------------|-------------------|---------------------------------|--------------------------------|------------------------------|
| | | α, α' | β, β' | γ, γ' | $\alpha\beta, \alpha'\beta'$ | $\alpha\gamma, \alpha'\gamma'$ | $\beta\gamma, \beta'\gamma'$ |
| $[\text{cis-PtCl}(\text{PEt}_3)_2(\text{naph})]^+ \text{ } ^b$ | -70 | ~9.25, ~9.25 | 7.96, 7.81 | 8.85, 8.66 | 5.3, 3.9 | c | 8.0, 7.9 |
| $\text{Cr}(\text{CO})_5(\text{naph})$ | -30 | 9.72, 9.32 | 7.75, 7.85 | 8.72, 8.64 | 5.2, 4.2 | 1.5, 1.8 | 8.1, 8.1 |
| $\text{W}(\text{CO})_5(\text{naph})$ | -40 | 10.08, 9.46 | 7.92, 8.00 | 8.99, 8.82 | 5.1, 4.1 | 1.6, 1.9 | 8.1, 8.2 |

^a α , β , and γ positions are labeled relative to the nitrogen atoms. Unprimed positions are adjacent to the "coordinated" nitrogen and primed positions are adjacent to the "noncoordinated" nitrogen (see structures III and IV in the text and ref 18). ^b Data from ref 6. ^c Not resolved.



Figure 1. ^1H NMR spectra for $[\text{Cr}(\text{CO})_5(\text{naph})]$ recorded at 250 MHz in the temperature range 243-303 K. The right-hand plots are observed spectra and the left-hand plots are computer simulations. Peaks marked \times are due to an impurity and to some decomposition at the higher temperatures.

(structure IV). For naph some degree of interaction with the second nitrogen is possible in the solid state, and the precise definition of the structure must await an X-ray study. However, it is clear that in solution the two rings are not equivalent,

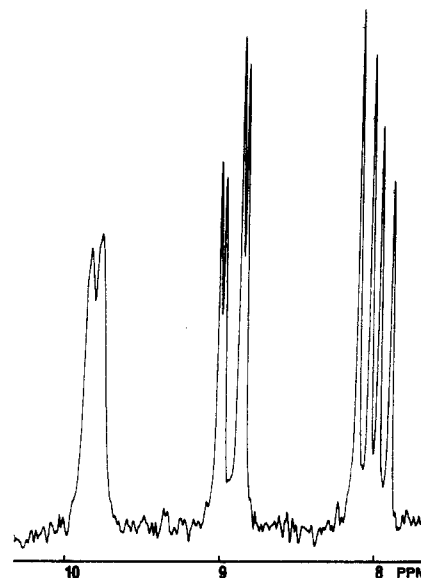


Figure 2. Fast-exchange limiting ^1H NMR spectrum for $[\text{W}(\text{CO})_5(\text{naph})]$ recorded at 60 MHz at 300 K.

with the ligand bound unsymmetrically in the static structure. Below -40°C both $[\text{M}(\text{CO})_5(\text{naph})]$ complexes (acetone- d_6 solution) show six well-resolved proton signals (Figure 1) assigned to the two AMX spin systems $\alpha\beta\gamma$ and $\alpha'\beta'\gamma'$. The chemical shifts and coupling constants are collected in Table II together with comparable data⁶ for $[\text{cis-PtCl}(\text{PEt}_3)_2(\text{naph})][\text{BF}_4]$. The naph bonding in the latter is known to approach monodentate geometry with Pt-N lengths of 2.08 and 3.05 Å. The coordinated ($\alpha\beta\gamma$) and noncoordinated¹⁸ ($\alpha'\beta'\gamma'$) ring resonances have been distinguished primarily on the basis of the earlier results,⁶ which showed that $J_{\alpha\beta} > J_{\alpha'\beta'}$. This established the α, α' assignments, and the remainder follow from the mutual coupling relationships. It is clear that the NMR parameters for $[\text{M}(\text{CO})_5(\text{naph})]$ are very similar to those in the Pt complex and a similar mode of coordination, i.e., IV, may be assumed for the naph ligand.

Raising the temperature of solutions of $[\text{M}(\text{CO})_5(\text{naph})]$ causes the series of NMR spectral changes illustrated in Figure 1 for $\text{M} = \text{Cr}$. This results in a high-temperature-limit spectrum like that illustrated in Figure 2 for $\text{M} = \text{W}$, in which only a single AMX pattern is distinguishable, indicating that the $\alpha\beta\gamma$ and $\alpha'\beta'\gamma'$ nuclei are being rendered equivalent by

rapid metal exchange between the two nitrogen atoms. Computer simulation of the line shapes at various temperatures (illustrated in Figure 1 for $M = \text{Cr}$, line width 1.5 Hz) leads to the thermodynamic parameters listed in Table I by use of the same method as was described above for the phth complexes. The naph system has the advantage that the more complex spin system facilitates reliable line shape fitting at the temperature extremes (i.e., well above and below the coalescence temperature), whereas the simple singlet spectra of the phth complexes permit good fitting only in the coalescence region.

Discussion

As noted at the beginning of this paper, previous detailed studies of metal site exchange in naph complexes have been limited to the essentially square-planar species $[\text{AuX}(\text{CH}_3)_2(\text{dmnaph})]$ and $[\text{cis-MCl}(\text{PR}_3)_2(\text{naph})]^+$, $M = \text{Pt}$ and Pd .^{6,7} These investigations led to the conclusion that the most likely mechanism for dynamic behavior is an intramolecular process for which the transition state involves naph bound to the metal via both nitrogens as a symmetric chelate. In the case of the platinum complexes dissociative mechanisms involving metal-nitrogen bond cleavage can be specifically excluded since ^{195}Pt - ^1H spin-spin coupling is distinguishable at the fast-exchange limit⁶ whereas for the more labile palladium complexes there is evidence that both intramolecular and dissociative processes occur.⁷ In $[\text{cis-PtCl}(\text{PEt}_3)_2(\text{phth})]^+$, ^{195}Pt - ^1H coupling is not maintained at the fast-exchange limit and a dissociative mechanism is indicated.⁶ The observed activation energies ($\Delta G^\ddagger_{T_c}$) at the coalescence temperatures (T_c) reflect these mechanistic differences with the intramolecular process in naph complexes ($\sim 44 \text{ kJ mol}^{-1}$ for Au, $\sim 51 \text{ kJ mol}^{-1}$ for Pt) being more facile than the dissociative process in phth complexes ($\sim 76 \text{ kJ mol}^{-1}$). The ΔG^\ddagger_{298} values shown in Table I for the $[\text{M}(\text{CO})_5\text{L}]$ complexes, $L = \text{naph}$ or phth , are thus closely comparable with the literature data for Au and Pt complexes, suggesting that a similar mechanistic interpretation may be appropriate; however, insufficient data are yet available relating to either intra- or intermolecular exchange involving M - N bonds to comment meaningfully on the fact that the ΔG^\ddagger_{298} values are near-identical for $M = \text{Cr}$ or W complexes of each of the ligands under discussion.

The results for phth complexes in Table I may also be compared with those for a series of $[(\text{aryl})\text{Cr}(\text{CO})_2(2,3\text{-diazabicyclo}[2.2.1]\text{hept-2-ene})]$ complexes¹⁰ and with those for the Cr and W complexes^{11,12} $[\text{M}(\text{CO})_5(\text{benzo}[c]\text{cinnoline})]$. For the first type, activation energies ($\Delta G^\ddagger_{T_c} = 71.1\text{--}82.8 \text{ kJ mol}^{-1}$) are similar to those in Table I for phth complexes, and while an intramolecular process was assumed, the only evidence appears to be the reversibility of the variable-temperature spectra¹⁰ and a dissociative process seems equally likely. In the benzo[*c*]cinnoline case, no thermodynamic parameters were calculated but since a dynamic process is already fast for the Cr complex at ambient temperature^{11,12} a lower activation energy is likely: it has been suggested that this is associated with low-lying $\pi^*(\text{N}=\text{N})$ orbitals.¹² There is, however, disagreement over the rate in $[\text{W}(\text{CO})_5(\text{benzo}[c]\text{cinnoline})]$, one group reporting it to be fluxional at ambient temperature¹² and the other rigid.¹¹ The reason for this conflict is not clear, but it seems possible that the complexes are difficult to obtain pure.

Experimental Section

Data relating to the characterization of the complexes are given

in the Results section and in the preparative descriptions below. Microanalyses were by Canadian Microanalytical Service Ltd., Vancouver, BC. Melting points were determined in open capillary tubes. Mass spectra were recorded with a Perkin-Elmer/Hitachi RMU 7E unit. IR spectra were recorded from 5000 to 200 cm^{-1} with an accuracy of 3 cm^{-1} on a Perkin-Elmer Model 283 spectrophotometer. Solid samples were examined as Nujol mulls between CsI plates. ^1H NMR spectra were recorded at 90 MHz on a Perkin-Elmer R32 spectrometer and at 250 MHz on a Bruker WP 250 Fourier transform spectrometer. NMR solvents were dioxane for the phth complexes and acetone-*d*₆ for the naph complexes with SiMe_4 as internal reference in both cases. Simulated NMR spectra were calculated on an IBM 3031 computer and plotted on a Tektronix 4013 graphics screen for preliminary work or a Calcomp 1039 drum plotter for final data. The programs used were a locally constructed package based on DNMR3¹⁴ for dynamic spectra and UEAIR¹⁵ and NMRPLOT¹⁶ for static spectra, iterative refinement, and plotting.

All manipulations were carried out under an atmosphere of dry nitrogen with use of Schlenk tube techniques. Solvents were dried by appropriate methods and distilled under nitrogen prior to use. $\text{Cr}(\text{CO})_6$ (Strem Chemicals Inc.), $\text{Mo}(\text{CO})_6$ (Alfa-Ventron Corp.), $\text{W}(\text{CO})_6$ (Strem Chemicals Inc.), and phthalazine (Aldrich Chemical Co.) were commercially available and were used as received. 1,8-Naphthyridine was prepared as previously described¹⁷ as were its complexes⁸ $[\text{M}(\text{CO})_5(\text{naph})]$, $M = \text{Cr}$ and W .

$\text{W}(\text{CO})_5(\text{phth})$. A solution of $\text{W}(\text{CO})_6$ (0.184 g, 0.52 mmol) in tetrahydrofuran (100 mL) was irradiated in a Pyrex glass tube for 8 h with a Hanovia 450-W UV lamp. Phthalazine (0.068 g, 0.52 mmol) in tetrahydrofuran (10 mL) was added, and the initially yellow solution changed to red. The mixture was stirred overnight, during which time the color returned to yellow; solvent was removed in vacuo and unreacted $\text{W}(\text{CO})_6$ removed by sublimation. The residue was recrystallized from 1:4 THF/hexane at $-25 \text{ }^\circ\text{C}$ to give $\text{W}(\text{CO})_5(\text{phth})$ as an orange-brown microcrystalline solid (0.17 g, 0.37 mmol), mp $130\text{--}140 \text{ }^\circ\text{C}$ dec. Anal. Calcd for $\text{C}_{13}\text{H}_6\text{N}_2\text{O}_5\text{W}$: C, 34.39; H, 1.33; N, 6.17. Found: C, 34.30; H, 1.39; N, 5.66.

$\text{Cr}(\text{CO})_5(\text{phth})$. A similar procedure using $\text{Cr}(\text{CO})_6$ (0.30 g, 1.36 mmol) in methanol (30 mL) with phthalazine (0.177 g, 1.36 mmol) yielded $\text{Cr}(\text{CO})_5(\text{phth})$ as orange-yellow crystals (0.22 g, 0.68 mmol), mp $130\text{--}135 \text{ }^\circ\text{C}$ dec. Anal. Calcd for $\text{C}_{13}\text{H}_6\text{N}_2\text{O}_5\text{Cr}$: C, 48.46; H, 1.88; N, 8.70. Found: C, 49.28; H, 1.44; N, 8.67.

Acknowledgment. We thank the NSERC, Canada, and the University of Victoria for financial support.

Registry No. $\text{Cr}(\text{CO})_5(\text{phth})$, 83061-16-9; $\text{W}(\text{CO})_5(\text{phth})$, 83061-17-0; $\text{Cr}(\text{CO})_5(\text{naph})$, 41119-94-2; $\text{W}(\text{CO})_5(\text{naph})$, 41119-95-3.

- (14) D. A. Kleier and G. Binsch, *QCPE*, **165** (1969).
 (15) R. B. Johannsen, J. A. Ferretti, and R. K. Harris, *J. Magn. Reson.*, **3**, 84 (1970).
 (16) J. D. Swalen in "Computer Programmes for Chemistry", Vol. 1, D. F. Detar, Ed., W. A. Benjamin, New York, 1968.
 (17) W. W. Paudler and T. J. Kress, *J. Org. Chem.*, **32**, 832 (1967).
 (18) The term noncoordinated is used here only to distinguish between the two rings in the naph skeleton and is not intended to exclude the possibility of a weak interaction between the metal and the more distant nitrogen atom.

Contribution from the Inorganic Chemistry and Crystallography Departments, University of Nijmegen, Toernooiveld, 6525 ED Nijmegen, The Netherlands

Gold Clusters.

Tetrakis[1,3-bis(diphenylphosphino)propane]hexagold Dinitrate: Preparation, X-ray Analysis, and ^{197}Au Mössbauer and $^{31}\text{P}\{^1\text{H}\}$ NMR Spectra

J. W. A. van der Velden, J. J. Bour,* J. J. Steggerda, P. T. Beurskens, M. Roseboom, and J. H. Noordik

Received November 20, 1981

Gold cluster compounds are of interest because of their remarkable structures but also because of the rather fast in-

- (10) M. Herberhold, K. Leonhard, and C. G. Kreiter, *Chem. Ber.*, **107**, 3222 (1974).
 (11) M. Kooti and J. F. Nixon, *J. Organomet. Chem.*, **105**, 217 (1976).
 (12) C. C. Frazier III and H. Kisch, *Inorg. Chem.*, **17**, 2736 (1978).
 (13) G. W. Bushnell, K. R. Dixon, D. T. Eadie, and S. R. Stobart, *Inorg. Chem.*, **20**, 1545 (1981), and references therein.